



LAWRENCE
LIVERMORE
NATIONAL
LABORATORY

Advances in Target Design for Heavy-Ion Fusion

D. A. Callahan, M. Tabak, G. R. Bennett, M. E. Cuneo,
R. A. Vesey, A. Nikroo, D. Czechowicz, D. Steinman

June 22, 2005

32nd European Physical Society Plasma Physics Conference
Barcelona, Spain
June 27, 2005 through July 1, 2005

Disclaimer

This document was prepared as an account of work sponsored by an agency of the United States Government. Neither the United States Government nor the University of California nor any of their employees, makes any warranty, express or implied, or assumes any legal liability or responsibility for the accuracy, completeness, or usefulness of any information, apparatus, product, or process disclosed, or represents that its use would not infringe privately owned rights. Reference herein to any specific commercial product, process, or service by trade name, trademark, manufacturer, or otherwise, does not necessarily constitute or imply its endorsement, recommendation, or favoring by the United States Government or the University of California. The views and opinions of authors expressed herein do not necessarily state or reflect those of the United States Government or the University of California, and shall not be used for advertising or product endorsement purposes.

Advances in Target Design for Heavy-Ion Fusion

D. A. Callahan¹, M. Tabak¹, G. R. Bennett², M. E. Cuneo², R. A. Vesey², A. Nikroo³, D. Czechowicz³, D. Steinman³

¹ Lawrence Livermore National Laboratory, Livermore, CA, USA

² Sandia National Laboratories, Albuquerque, NM, USA

³ General Atomics, San Diego, CA USA

Abstract

Over the past few years, the emphasis in heavy ion target design has moved from the distributed radiator target to the “hybrid” target because the hybrid target allows a larger beam focal spot than the distributed radiator (~ 5 mm radius rather than ~ 2 mm radius). The larger spot relaxes some of the requirements on the driver, but introduces some new target physics issues. Most notable is the use of shine shields and shims in the hohlraum to achieve symmetry rather than achieving symmetry by beam placement.

The shim is a thin layer of material placed on or near the capsule surface to block a small amount of excess radiation. While we have been developing this technique for the heavy ion hybrid target, the technique can be used in any indirect drive target. We have begun testing the concept of a shim to improve symmetry using a double-ended z-pinch hohlraum on the Sandia Z-machine. Experiments using shimmed thin wall capsules have shown that we can reverse the sign of a P_2 asymmetry and significantly reduce the size of a P_4 asymmetry. These initial experiments demonstrate the concept of a shim as another method for controlling early time asymmetries in ICF capsules.

Introduction

An accelerator producing a beam of heavy ions is an attractive driver for an inertial fusion energy plant. Accelerators have the long lifetime (~ 30 years), high repetition rates (~ 5 -10 Hz), and high efficiency (~ 25 -40%) needed for a power plant. In addition, the final focus is done by magnetic fields so that the final optic (magnet) can be protected from neutron damage.

The accelerator is the most expensive part of a heavy-ion fusion power plant. As such, anything that can be done to reduce the cost of the accelerator has a direct impact on the cost of the plant and the final cost of electricity. So, to make heavy-ion fusion attractive, we need to find ways to reduce the cost of the driver.

One of the things that sets the size of the accelerator is the size of the spot that is needed at the target. The important parameter from the target perspective is the amount of material that is needed to stop the ion beam. Hence, the ion mass and ion kinetic energy can be changed as long as the total ion range is kept constant. The beam current, however, scales inversely with the ion kinetic energy so that we need a larger current if we use a lower mass, lower kinetic energy ion. So, a lower mass, lower kinetic energy ion allows a shorter, cheaper accelerator, but the beam is more difficult to focus.

Hybrid Target Design

To relax the requirements on beam focusing, we have designed a target with a larger beam spot than our previous designs. We call this design a “hybrid” target because it is a hybrid of our distributed radiator designs [1,2] and the end radiator design of Ho [3]. It is similar to the “foam target” of Honrubia [4].

The hybrid target is shown in Figure (1). Two-dimensional, integrated Lasnex calculations of the hybrid target produce 370 MJ of energy from 6.7 MJ of beam energy (the 1-d yield for this pulse shape is 410 MJ). This represents a target gain of 55. These calculations assume the beams have a Gaussian distribution and are elliptical with semi-major and semi-minor axes of 5.4 by 3.8 mm (this ellipse contains 95% of the beam energy). As with our other heavy ion target designs, the ion kinetic energy is changed from the foot to the main pulse to compensate for range shortening as the target heats. This can be accomplished by using different beams for the foot and main pulse. The foot beams (with the lower kinetic energy) are removed from the accelerator at the appropriate energy and then drift to the target while the main pulse beams continue to be accelerated. In the calculations, the foot beams were assumed to be 3 GeV Pb in a 6 degree cone. The main pulse beams were assumed to be 4.5 GeV Pb beams in a 12 degree cone.

The basic idea of this target is to illuminate the entire end of the hohlraum with the ion beam. Since the ion beam has a distribution that is peaked in the center (a Gaussian was used in these calculations), most of the energy (> 50%) is deposited near the axis of the hohlraum. If we did nothing to correct the location of the energy deposition, the capsule would “see” a very hot source near the capsule pole and the resulting implosion would be too high on the pole and result in an oblate (“pancaked”) implosion. To correct this lowest order asymmetry (a P_2 Legendre mode), we put a shield between the ion beam radiation converter and the capsule. In this case, the shield was made of tin and designed to be a few mean-free-paths thick in order to block the capsule’s view of most of the radiation coming from the converter.

The radiation then flows around the shield to the capsule. The hohlraum is designed so that radiation flowing around the shield is near the zero of P_2 . Unfortunately, the zero of P_2 is near the peak of negative P_4 . Uncorrected, this will also lead to a non-spherical implosion that will not ignite.

We fix this asymmetry using a shim, which is a small amount of material placed on or near the capsule surface to block a small amount of excess radiation. By putting the shim close to the capsule, we benefit from radiation transport smoothing so that the perturbation is small. This means that a relatively small amount of material is needed to correct the asymmetry and the energy penalty is also small. The downside of placing the shim close to the capsule is that it can only correct asymmetries early in the pulse. Later in the pulse, the thin layer will burn through and be pushed away from the capsule by the ablator material and so it will effectively disappear. This is still a useful technique, however. Often, the asymmetry is largest early in the pulse because the hohlraum walls are still cold. The contrast between the cold walls and the source of radiation is large. Later in time, the walls heat up so the perturbation is effectively

smaller. In addition, late in time, the capsule starts to shrink so that the asymmetry is further reduced by radiation transport smoothing.

Experimental Test of Shims

Using a shim to correct an asymmetry is key to the hybrid target. If we cannot correct the P_4 asymmetry using the shim, then we would need to make the hohlraum larger in order to depend on radiation transport smoothing. Since about half the energy ends up in hohlraum wall, this can result in a considerable energy penalty and reduction in target gain.

The double z-pinch target [5,6,7] uses similar methods to the hybrid target for achieving symmetry. In the double z-pinch target, two z-pinches sit at the ends of the hohlraum and produce radiation to drive a capsule. Like the hybrid target, a shield is used to block the capsule's view of the radiating pinches. Again, like the hybrid target, radiation flows around the shield near the zero of P_2 and, with a small enough case-to-capsule ratio, the resulting implosion suffers from a negative P_4 asymmetry. Since the heavy ion target and the z pinch target have similar symmetry issues and since a heavy ion accelerator that is capable of heating a target to 70-100 eV will not be available for many years, we take advantage of this natural area of collaboration and test the concept of shims on the Z facility at Sandia National Laboratory.

The first tests of shims were to show that symmetry can be changed using a shim. To do so, we use 4.7 mm diameter, thin-shelled capsule (27 microns thick CH doped with 2% Ge) and use a backlighter to measure the asymmetry as the capsule implodes. Our first experiments are designed to show that the basic principle of the shim can work; that the shim can change the asymmetry of the capsule.

We begin by doing "null" experiments without the shim to measure the asymmetry. The imploding shell is imaged using 6.7 keV photons. Figure (2) shows the image of the shell – which has the characteristic diamond shape of a negative P_4 asymmetry. Finding the radius of minimum transmission, we can plot the radius of the shell as a function of angle, which is shown in Figure (3). We see that even though the convergence ratios are small (~ 1.7 and 2), the distortions are large (> 100 microns). If we decompose the radius into Legendre moments, then we find that Z1373, there is a $+2.8\%$ P_2 and a $+4.5\%$ P_4 in the shell. (Note that a negative P_4 asymmetry in the radiation drive results in a positive P_4 asymmetry in the shell radius.)

Figure (3) also shows the radius versus angle for a simulated radiograph of this experiment. In the calculations, a temperature asymmetry is imposed on the capsule. We vary this asymmetry until we get good agreement with the experiment; that same asymmetry is then used in the calculations that include the shim layer.

The shim layer was designed to take out the P_4 asymmetry. To fabricate the angle-dependent layer, the capsule was mounted on a 200 micron diameter tungsten stalk. The capsule was then rotated under a coater, which added a thin layer of gold. A mask was used to tailor the layer to the desired profile. Once the layer is in place, the capsule is radiographed to measure the layer thickness as a function of angle. Two views of the

capsule must be used – one near the equator and one near the pole – because it becomes difficult to measure the layer thickness as the view becomes more and more tangent to the capsule surface. The measured thickness of the layer is shown in Figure (4). The two separate pieces of data are those that come from the equator and pole views. There is a gap between these two pieces of data – between 42 and 55 degrees. Figure (4) shows the fit to the data that was used in the calculations.

Figure (5) shows the radiographs of the capsules with the shim layer. The images are visibly rounder than those without the shim layer. Figure (6) shows the radius of the shell versus angle. A Legendre decomposition of the shell radius for shot Z1379 (which is at nearly the same convergence ratio as shot Z1373) shows that we have reduced the P_4 asymmetry from +4.5% to +1.6%. Interestingly, the data also shows that we have flipped the sign of the P_2 asymmetry from +2.8% without the shim to -2.1% with the shim.

Calculations using the shim layer shown in Figure (7) produce simulated radiographs that are visibly rounder than those without the shim layer. When we plot the radius versus angle for the simulated radiographs and compare them to the data, we find a discrepancy (shown in Figure (8)). Near the capsule waist (90 degrees and 270 degrees), the data and simulations do not agree. A Legendre decomposition of the simulated radiographs quantifies this discrepancy. The data and the simulation both show a reduction in the P_4 asymmetry: -1.1 % for the simulation with the shim, +1.6% for the experiment with the shim compared to +4.5% without the shim. However, the simulation shows virtually no change in P_2 , while the experiment showed a reversal in P_2 (+2.3% for the simulation with the shim, -2.1% for the experiment with the shim compared to +2.8% for the experiment without the shim).

One possible explanation for this discrepancy is that the layer profile used in the calculations is not accurate. If we look at the data in Figure (4), we notice that the two pieces of data do not appear to meet in the gap between 42 and 55 degrees. The error bars on the radiograph of the layer are +/- 10%. To see if it is possible for this to explain the discrepancy, we take the limit of those error bars and try thickening the layer by 20% at the waist. The “adjusted data” is shown in figure (9). By adjusting the thickness near the waist, we note that it now appears that the two pieces of data meeting in the gap between 42 and 55 degrees. We fit this “adjusted data” using the curve shown in figure (9) and rerun the calculations.

The results are shown in figure (10). The radius versus angle now agrees fairly well with the data. The Legendre decomposition of the radius for the simulation of shot Z1379 now shows a reversal in P_2 (-1.2% for the simulation with the “adjusted” layer compared to -2.1% for the experiment) and a reduction in P_4 (-0.8% for the simulation with the “adjusted” layer compared to 1.6% for the experiment). These results suggest that the discrepancy between the simulation and data is due to inaccurate characterization of the layer; we are currently working on developing other techniques for characterizing the layer that may confirm this suspicion.

These experiments have demonstrated that we can change capsule symmetry using a shim layer. By varying the thickness of the shim layer, we expect that we will be able to zero and reverse P_4 ; future experiments will measure the asymmetry as a function of shim thickness. This is the first step in developing this technique—which should be applicable to any indirect drive target. The next step is to understand why the P_2 symmetry changed. Beyond that, we need to understand the implications of the shim layer on short wavelength perturbations.

Conclusions

An accelerator producing a beam of heavy ions has many attractive features as a driver for an inertial fusion energy power plant. Accelerators have the long lifetime (~ 30 years), high repetition rate ($\sim 5 - 10$ Hz), and high efficiency ($\sim 25-40\%$) needed for a power plant. In addition, the final focusing is done by magnetic fields so that it is possible to protect the final optic (magnet) from damage due to neutrons and debris. To make heavy ion fusion competitive with other sources of energy, we always need to be looking for ways to reduce the cost of the driver. Since the driver is the single most expensive part of the power plant, any reduction in the cost of the driver translates into a reduction of the capital cost of the plant and the cost of electricity.

One way to reduce the cost of the driver is to allow lower mass, lower kinetic energy ions. Lower kinetic energy translates into a shorter accelerator. As the ion kinetic energy is reduced, the amount of beam current needed to deliver the required power to the target increases. Larger beam currents are more difficult to focus onto a small spot and so targets that allow larger beam spots are highly desirable.

To meet this challenge, we have designed a “hybrid” target which allows a beam spot that is essentially the size of the hohlraum. While this makes the beam focusing easier, it also introduces new target physics issues since we now have to use internal hohlraum shields to control symmetry on the capsule. In particular, the hybrid target uses a shield to control P_2 asymmetry and a shim to control P_4 asymmetry.

These new symmetry techniques need to be tested experimentally. We have begun to test shims as a method for controlling early time symmetry using the double z-pinch hohlraum on the Z facility at Sandia. Our initial experiments are quite promising – showing a reduction in P_4 from 4.5% down to 1.6%. We expect that by increasing the thickness of the shim layer slightly, we could reduce the P_4 even further—future experiments will test thicker shim layers with the goal of zeroing and reversing P_4 . In addition, we are working on improved methods for characterizing the shim layers; we hope that better characterization will help us understand why we see a reversal in P_2 in the experiments.

Acknowledgements

This work performed under the auspices of the U.S Department of Energy by University of California, Lawrence Livermore National Laboratory under contract No. W-7405-Eng-48.

References

- [1] M. Tabak, D. A. Callahan-Miller, Phys. Of Plasmas, 5, 1895 (1998).
- [2] D. A. Callahan-Miller and M. Tabak, Nuclear Fusion, 39, 883 (1999).
- [3] D. D.-M. Ho, J. A. Harte, M. Tabak, Nuclear Fusion, 38, 701-710 (1998).
- [4] J. J. Honrubia, R. Ramis, J. Ramirez, J. Meyer-ter-Vehn, L. F. Ianez, A. R. Piriz, J. Sanz, M.M. Sanchez, M. De la Torre, Nucl. Inst. And Methods A, 415, 104-109 (1998).
- [5] J. H. Hammer, M. Tabak, S. C. Wilks, J. D. Lindl, D. S. Bailey, P. W. Rambo, A. Toor, G. B. Zimmerman, J. L. Porter, Phys of Plasmas, 6, 2129 (1999).
- [6] R. A. Vesey, M. E. Cuneo, J. L. Porter, R. G. Adams, R. A. Aragon, P. K. Rambo, L. E. Ruggles, W. W. Simpson, G. R. Bennett, Phys of Plasmas, 10, 1854 (2003).
- [7] G. R. Bennett, et. Al, Phys of Plasmas, 10, 3717 (2003).

Figure Captions:

Figure 1: A diagram of $\frac{1}{4}$ of the capsule and hohlraum for the hybrid target. The complete target is a rotation about the z-axis and a reflection about the r-axis. The materials and densities used were as follows: (A) AuGd at 0.1 g/cc, (B) 15 micron layer of AuGd at 13.5 g/cc, (C) Au at 32mg/cc, (D) $(CD_2)_{0.97} Au_{0.03}$ at 10 mg/cc, (E) AuGd at 0.1 g/cc, (F) $(CD_2)_{0.97} Au_{0.03}$ at 40 mg/cc, (G) AuGd at 0.1g/cc (upper half) and 0.2 g/cc (lower half), (H) CD_2 at 1 mg/cc, (I) Al at 55 mg/cc (lower half) and 121 mg/cc (upper half), (J) Sn at 0.2 g/cc (lower half) and 0.3 g/cc (upper half), (K) DT at 0.3 mg/cc, (L) DT at 0.25 g/cc, (M) $Be_{0.995}Br_{0.005}$ at 1.845 g/cc, (N) Al at 0.145 g/cc, (O) AuGd at 0.1 g/cc, (P) Fe at 10 mg/cc.

Figure 2: Radiographs of imploding shell on two shots (Z1372 and Z1373) shows the characteristic diamond shape of a P_4 asymmetry. The superimposed circle is to guide the eye. The convergence ratios for these shots are approximately 2 for Z1372 and 1.7 for Z1373.

Figure 3: The radius versus angle for the radiographs shown in figure (2) and for simulated radiographs of these experiments.

Figure 4: The measured thickness of the shim layer as a function of angle and the fit to that data that is used in the simulations

Figure 5: Radiographs of two experiments with the shim layer (Z1379 and Z1380). Both show a rounder implosion than without the shim (Figure 2). The superimposed circle is to guide the eye.

Figure 6: The radius versus angle for the experiments using the shim layer (shown in Figure 5). The shim layer has reduced the asymmetry from the case without the shim (Figure 3).

Figure 7: Simulated radiographs of the implosion with the shim layer also show a rounder implosion. The superimposed circle is to guide the eye.

Figure 8: The radius versus angle for the experimental radiographs and the simulated radiographs show some differences at the capsule waist (90 and 270 degrees).

Figure 9: Adjusting the shim layer by increasing the thickness by 20% at the waist.

Figure 10: Using the adjusted layer profile gives better agreement between the simulated and experimental radius versus time.

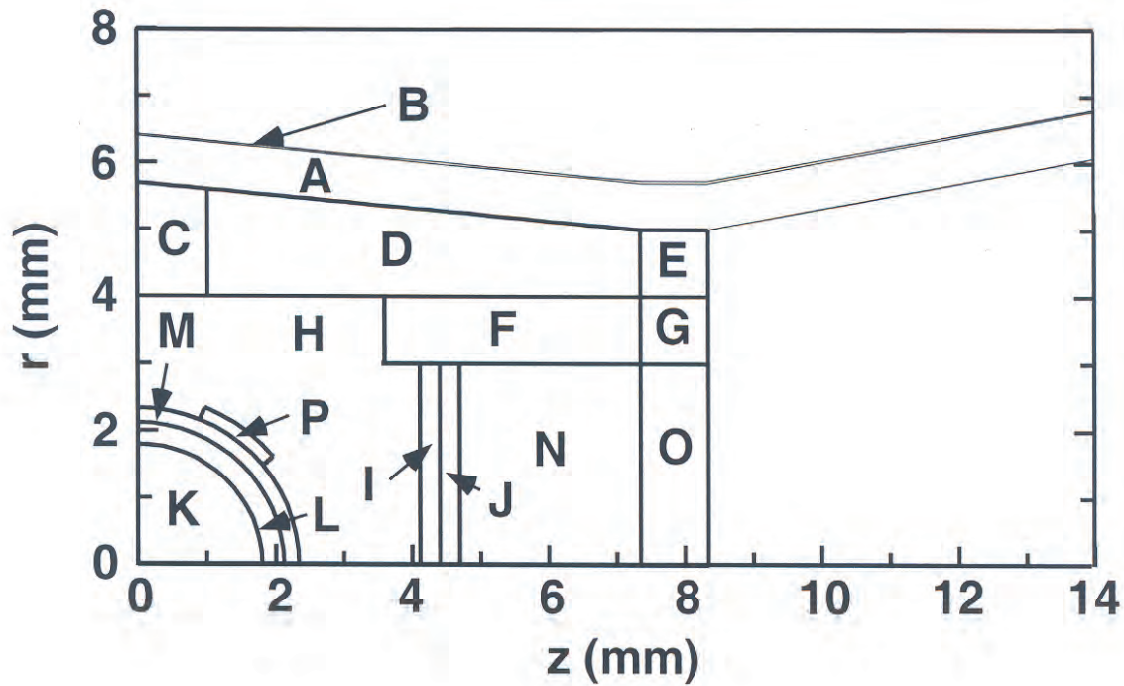


Figure 1

Z1372



Z1373

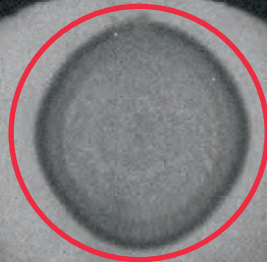


Figure 2

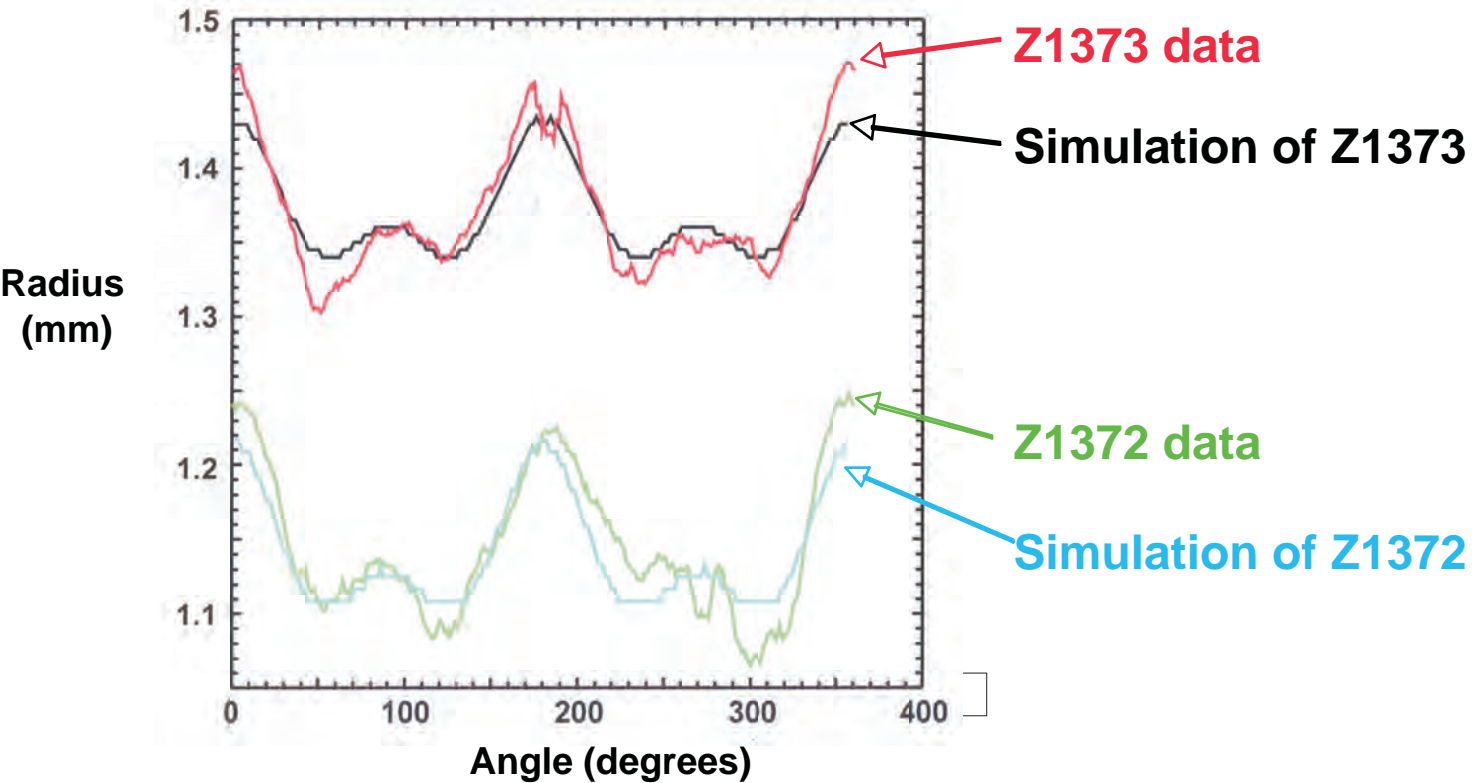


Figure 3

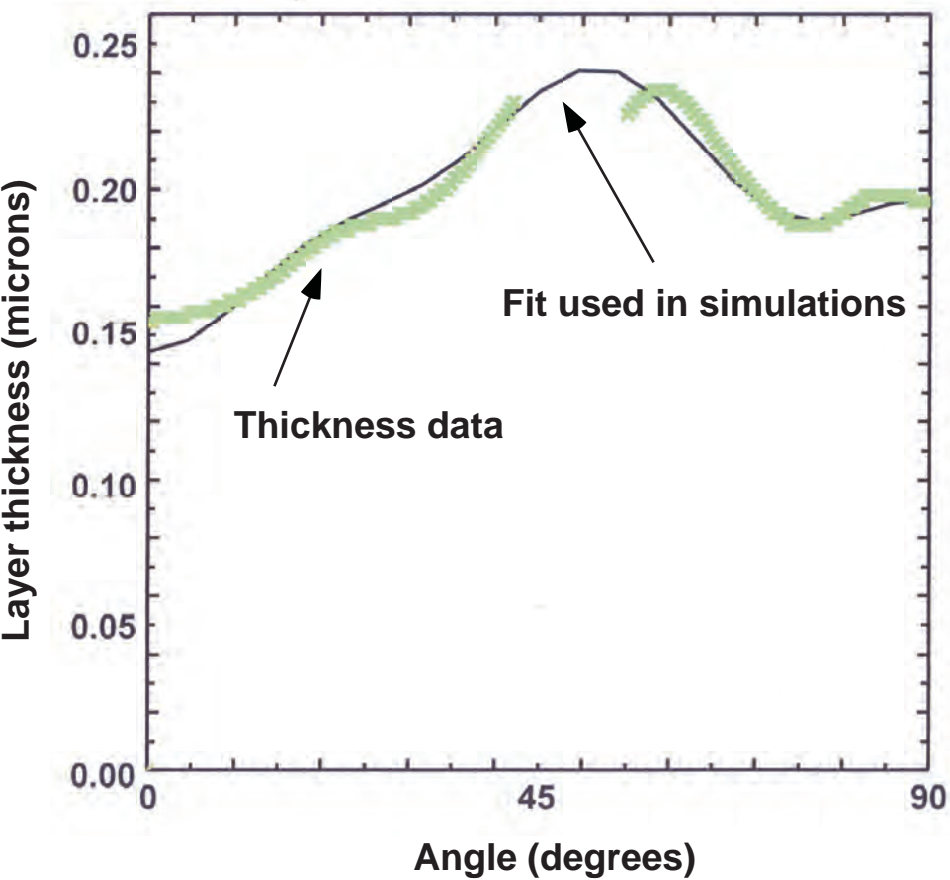
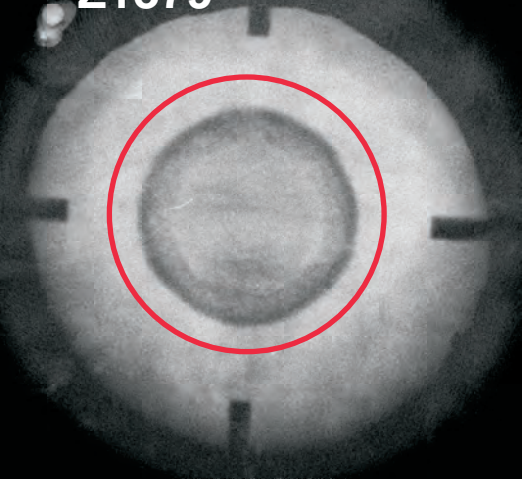


Figure 4

Z1379



Z1380

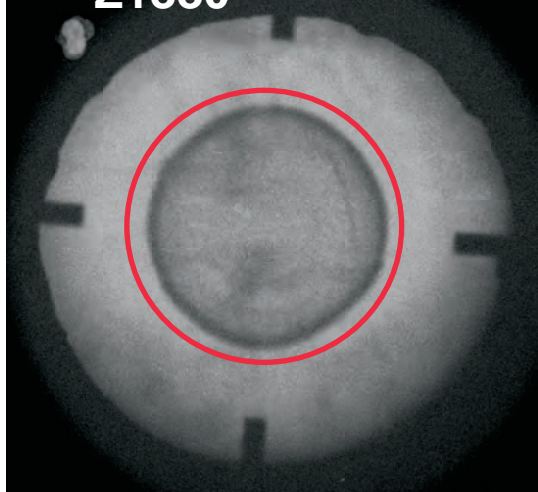


Figure 5

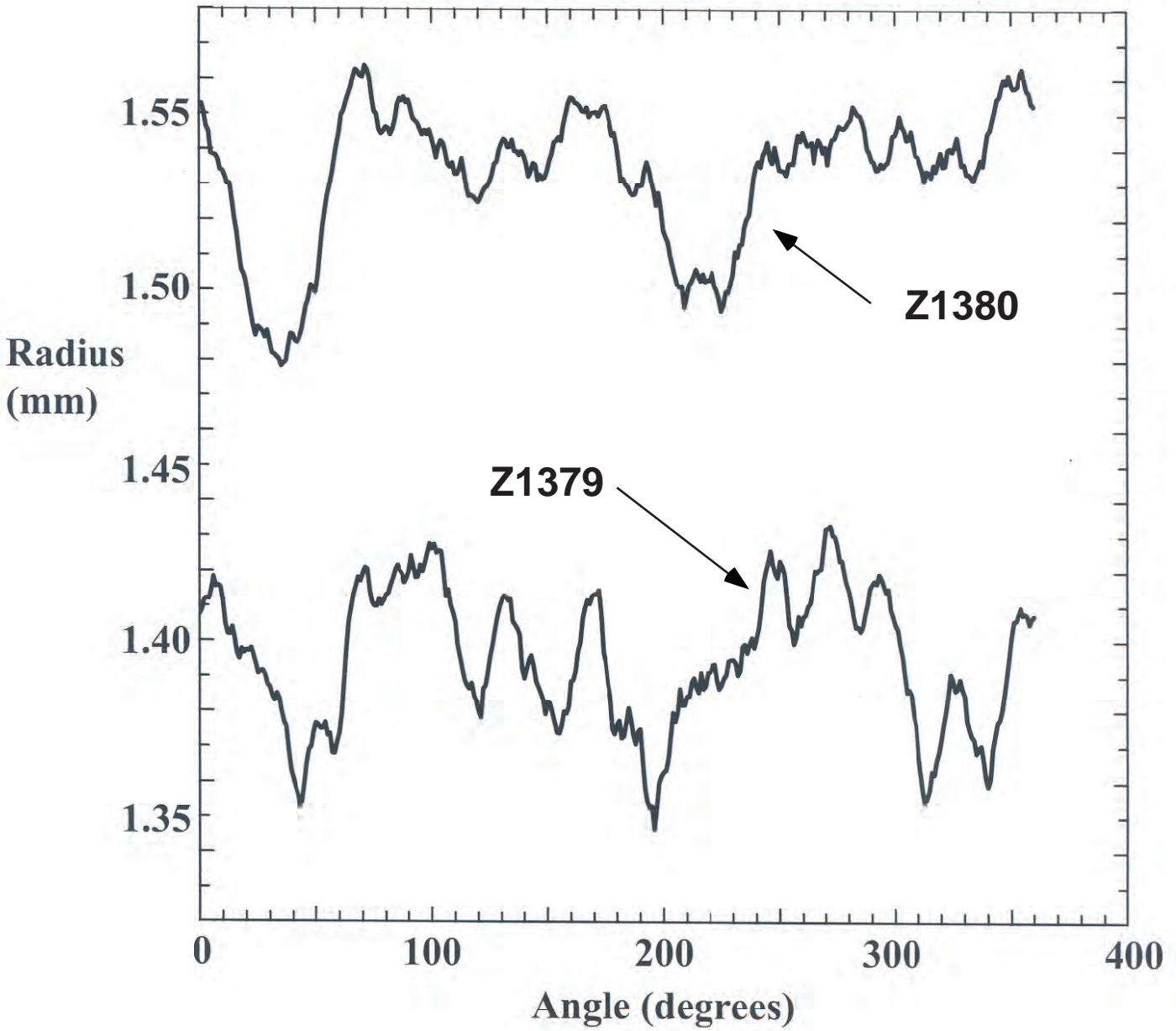


Figure 6

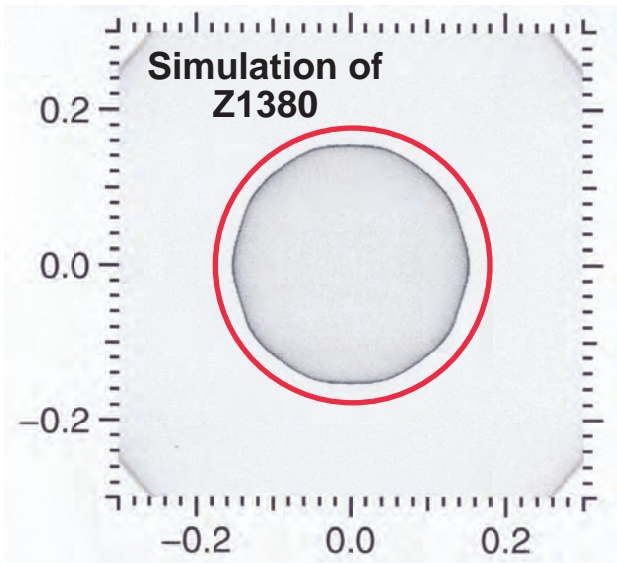
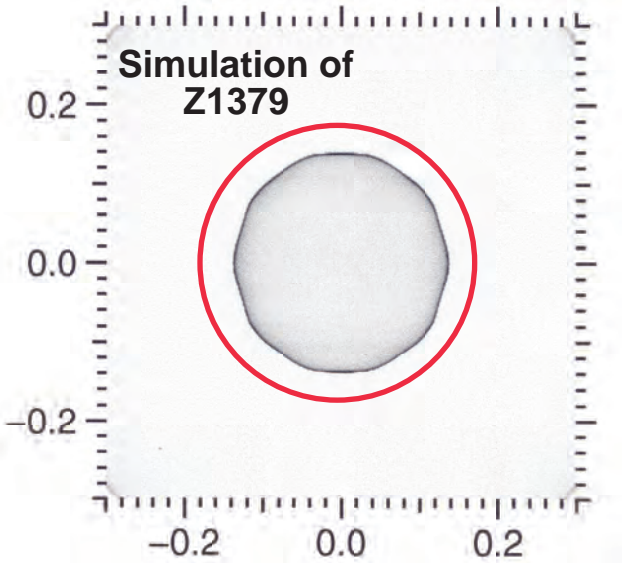


Figure 7

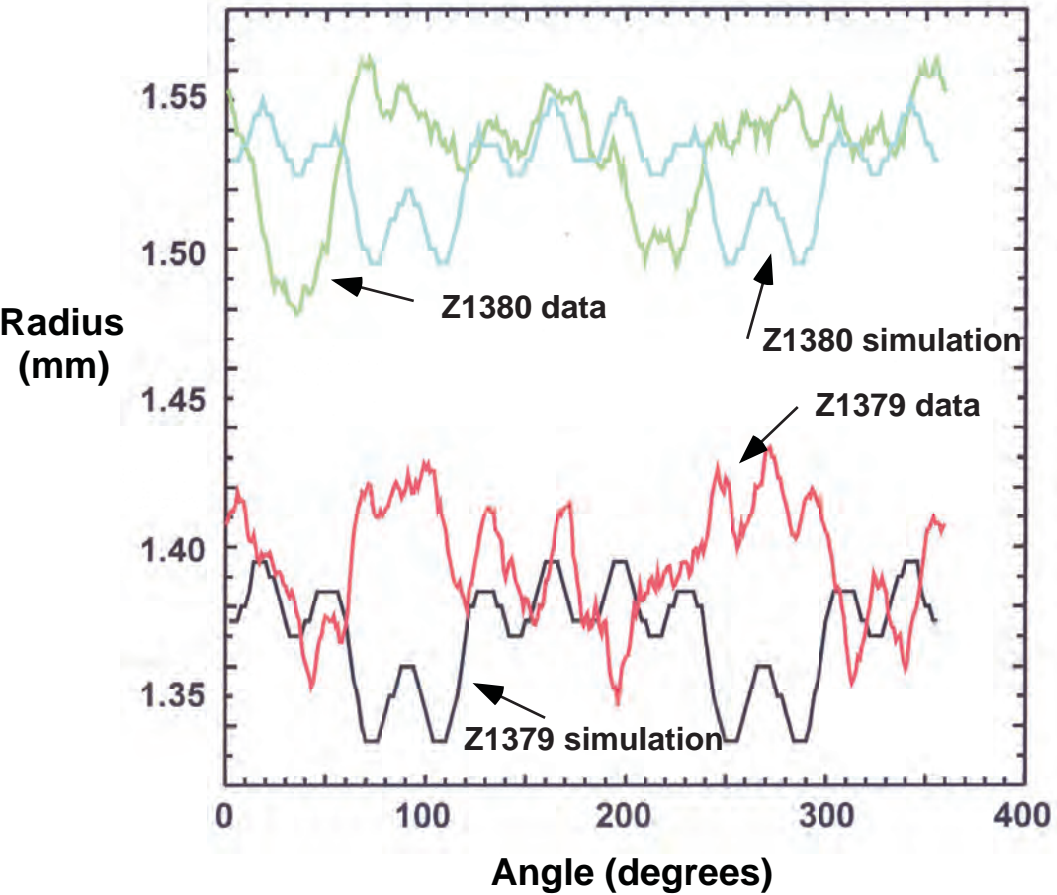


Figure 8

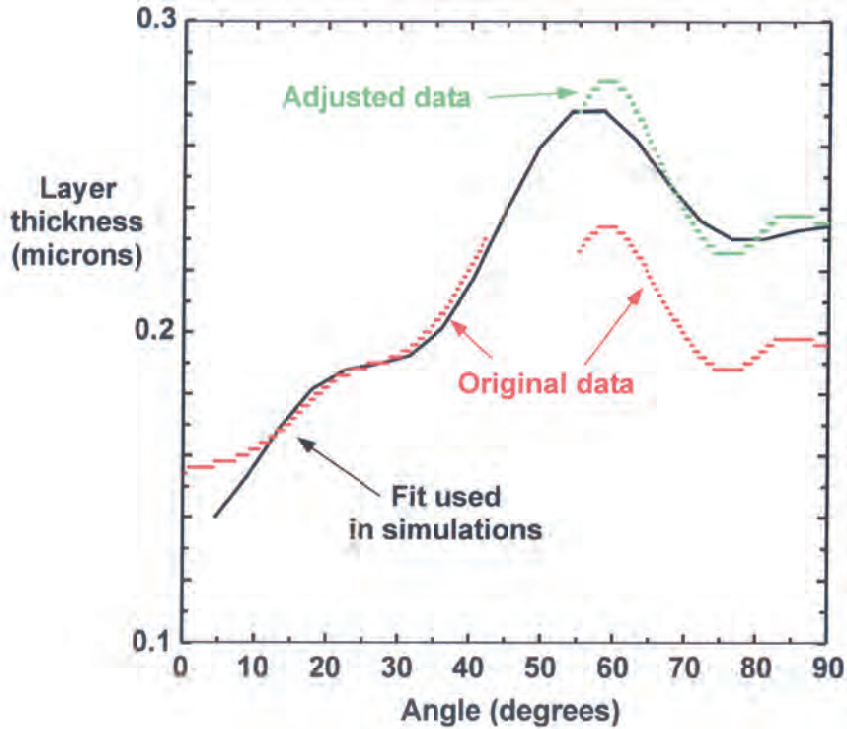


Figure 9

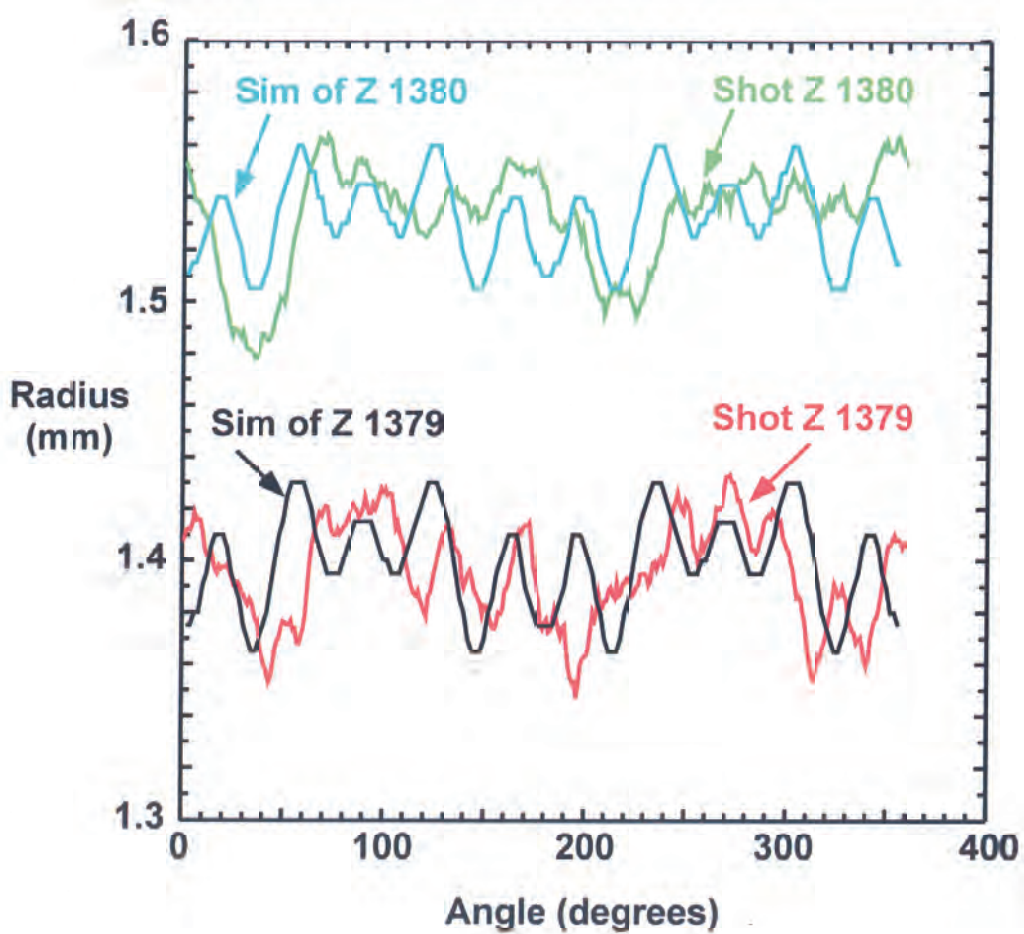


Figure 10